



Cargo Transportation and Methylene Blue Degradation by Using Fuel-Powered Micromotors

Zhonghao Li,^[a] Zhongzhou Xie,^[a] Hao Lu,^[a] Ying Wang,^{*,[a, b]} and Yongsheng Liu^{*,[a, b]}

In the past two decades, micromotors have experienced rapid development, especially in environmental remediation, the biomedical field, and in cargo delivery. In this study micromotors have been synthesized from a variety of materials. Different functional layers and catalytic layers are formed through template electrodeposition (the bottom-up method). At the same time, the article analyzes the influence of hydrogen peroxide concentration, surfactant type and concentration on

the speed of the micromotors. Cargo transportation through tubular micromotors has always been a problem that people are eager to solve. In this article, we electrodeposit a layer of Ni in the microtubes, which effectively guides the microtubular motors to complete the cargo transportation. The potential applications of micromotors are also being explored. We added the prepared micromotors to the methylene blue solution to effectively enhance the degradation.

1. Introduction

Great progress has been made on micromotors in the past two decades and designing new types of micromotors has become an important challenge. Multiple efforts are consistently made in the development of composition and structure of micromotors.

After decades of development, currently, the commonly used methods for preparing micro-nano motors mainly include template-assisted electrochemical deposition, crimping, metal chemical vapor deposition, physical vapor deposition, pickering emulsion.^[1] Compared with other methods, the template-assisted electrochemical deposition method is economical and convenient, suitable for mass preparation of micro-nano motors, and has good control over the size and shape of the motor.^[2] At the same time, this method also has the advantage of sequentially depositing different materials into the template holes, such as metals,^[3] polymers^[4] and 2D materials.^[5] A tubular micromotor driven by bubbles can be prepared by electrochemical deposition. Compared with electrophoresis propulsion^[6] and self-diffusion propulsion motors, bubble-propelled^[7] tubular micromotors have stronger propulsion

capabilities.^[8] Therefore, we prepared a series of different tubular micromotors for research. Because polyaniline(PANI) has conductivity^[9] and can be used to connect broken electronic components, gold (Au) and copper (Cu) have the function of local magnetic field enhancement and Raman scattering strength,^[10] so they are used as the functional layer of the micromotor. For the catalytic layer, we choose platinum (Pt) and silver (Ag). Pt has an excellent catalytic effect in the reaction with H₂O₂,^[11] but its high cost and easy deactivation are shortcomings, so we chose silver, which also has catalytic effect, as a substitute and comparison.

Studies have shown^[12] that in the movement of micromotors, the concentration of hydrogen peroxide, the type of surfactant and the concentration of surfactants have an important influence on it. In this article, we have carried out research on the influence of these three elements on the motion speed of the micromotor.


The use of micromotors to accomplish more complex tasks is highly anticipated. For example, micromotors have great prospects in the fields of biomedical applications^[13] and environmental remediation.^[11b,12b,14] In this article, we successfully guided the micromotor to contact the cargo by adding the magnetic metal Ni to the prepared micro-tubular motor, completing the transportation of the cargo. In addition, we also found that adding micromotors to the methylene blue solution can quickly complete the degradation of the methylene blue solution. This discovery provides a new way to explore the degradation of organic matter in the environment in the future.


2. Results and Discussion

Figure 1 describes the template preparation process of the microtubule engines. The microtubules prepared in this way look exactly like a miniature rocket. By changing the mode and rate of electrodeposition, the surface morphology and wall thickness of the microtubules can be controlled. The inside of the microtube is designed with a catalytic layer, so that a large

[a] Z. Li, Z. Xie, H. Lu, Prof. Y. Wang, Y. Liu
Department of Physics and Mathematics
Shanghai Key Laboratory of Materials Protection and
Advanced Materials in Electric Power
Shanghai University of Electric Power
Shanghai 201300 (China)
E-mail: 2006000081@shiep.edu.cn

[b] Prof. Y. Wang, Y. Liu
Department of Materials Science
Fudan University
Shanghai 200433 (China)
E-mail: yslu@shiep.edu.cn

 Supporting information for this article is available on the WWW under <https://doi.org/10.1002/open.202100064>

 © 2021 The Authors. Published by Wiley-VCH GmbH. This is an open access article under the terms of the Creative Commons Attribution Non-Commercial NoDerivs License, which permits use and distribution in any medium, provided the original work is properly cited, the use is non-commercial and no modifications or adaptations are made.

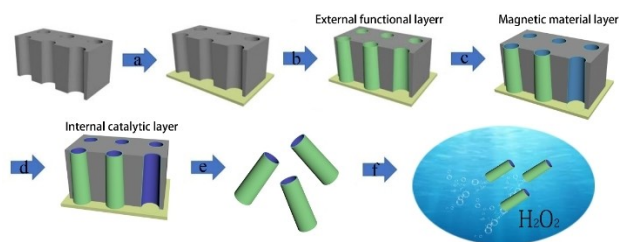


Figure 1. Schematic diagram of the steps of preparing microtubes by template-assisted electrodeposition. (a) Thermal evaporation to prepare a layer of gold. (b) Electrodeposition of the outer layer of microtubes. (c) Electrodeposition of the middle layer of microtubes. (d) Electrodeposition of the inner layer of microtubes. (e) Released in deionized water. (f) Observe movement in hydrogen peroxide solution.

number of bubbles are generated in the inner wall of the narrow tube, and the microjet is formed at the end of the microtube.^[15] Similar to the propulsion of rocket, bubbles in the walls of the microtubes provide a high level of propulsion for movement.^[16] Therefore, under lower hydrogen peroxide concentration, the microtubes can also move quickly. The membrane template assists electrodeposition through the porous structure of the membrane. Polyelectrolytes, metals, semiconductors, and carbon micro-nanorods or tubes can be synthesized by electrodeposition. There are a large number of monodispersed pore structures on the membrane. Each pore is equivalent to a separate reaction vessel. In this study, a polycarbonate membrane plate with a pore diameter of 5 μm was used. Figure 1 shows the step-by-step process of manufacturing microtubes by template electrodeposition (from a to f). First, a 75 nm Au layer on the surface of the template was evaporated by thermal evaporation, and then an external functional layer was deposited in the template. In this study, Au, Cu, and PANI were used. In order to achieve magnetic field control, a layer of metallic Ni was deposited continuously in the tube, along with an internal catalytic layer, so that the template could interact with the H_2O_2 solution to generate bubbles and push the micromotors forward. These processes are shown in steps b through d. After completing the above steps, the gold layer was completely removed by manually polishing it with 5 μm of alumina particles, and the film was dissolved in methylene chloride to release the micromotor. This is shown in step e. Finally, the movement of the motor in H_2O_2 aqueous solution was observed. This is demonstrated in step f.

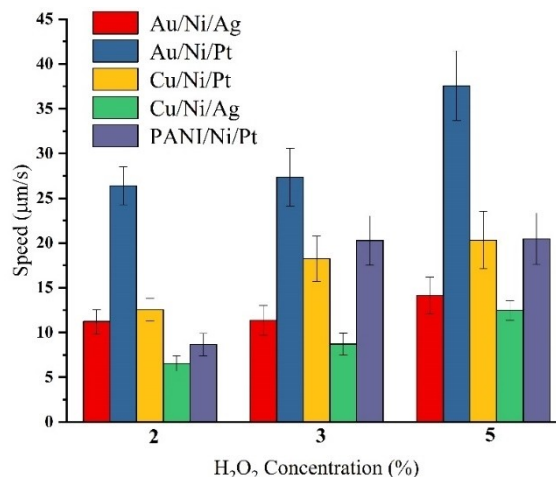


Figure 3. The movement speed of various types of microtubes at different concentrations of hydrogen peroxide. (Surfactants are all Triton X-100, the concentration is 1%)

Figure 2 shows the SEM and energy-dispersive spectroscopy (EDS) images of several microtube motors manufactured by this method, including PANI/Ni/Pt, Au/Ni/Ag, Cu/Ni/Pt, Cu/Ni/Ag, and Au/Ni/Pt motors. The SEM images in Figure 2 clearly reflect the growth morphology of the microtubes where the smooth outer surface is clearly observed. The EDS image shows that the elements are evenly distributed on the micromotor, reflecting good growth of the elements on the microtubes.

Figure 3 shows the movement speed of the five types of motors manufactured in different concentrations of H_2O_2 solution. The five types of micromotors are PANI/Ni/Pt, Au/Ni/Ag, Cu/Ni/Pt, Cu/Ni/Ag, and Au/Ni/Pt. Au, Cu, and PANI are the different outer layer materials for the micromotors. Au and Cu can be used in SERS area. PANI has good electrical conductivity. The fuel in the inner tube is made of Pt and Ag, as a comparison. Both metals can react with H_2O_2 solution very well. The surfactant added is 1% Triton X-100. While observing, the configured H_2O_2 solution was placed on a glass slide with a dropper, and a pipette was used to place the dispersed microtubes into it. Oxygen bubbles were generated at the tail of the microtube, pushing it forward. A video tracker was used to calculate the motor speed in this experiment. According to these experimental results, as the concentration of the H_2O_2 solution increased, the movement rate of the microtubes

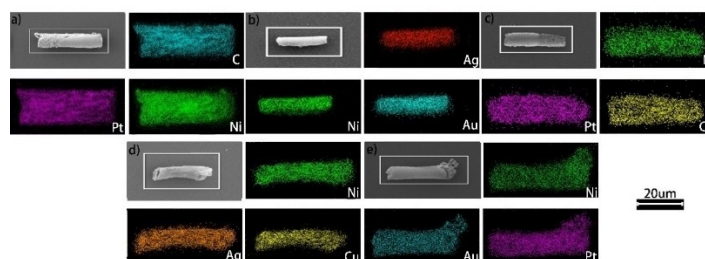


Figure 2. SEM and EDS images of prepared microtubes. (a) PANI/Ni/Pt (b) Au/Ni/Ag (c) Cu/Ni/Pt (d) Cu/Ni/Ag (e) Au/Ni/Pt

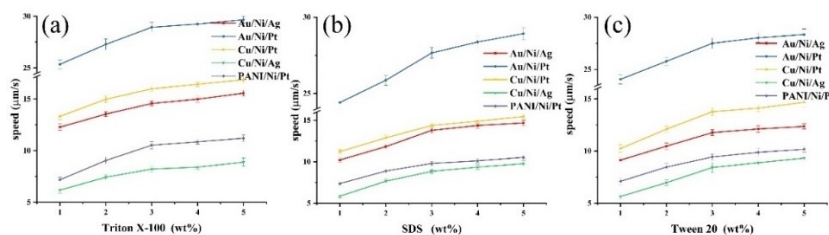


Figure 4. Curves of the velocity of various types of microtubules with concentration changes under different surfactants (H_2O_2 concentration is 2%). (a) Triton X-100 (b) SDS (c) Tween 20.

(regardless of type) also increased. Under the same external conditions, different kinds of microtubules have different velocities due to the influence of structural morphology, material and surface roughness.^[17] Under the same deposition conditions, the smooth surface helps to reduce resistance and enhance the detachment of bubbles from the surface of the microtubes.^[18] Since the electrochemically deposited gold has a smooth surface,^[19,20] under the same catalytic layer, with gold as the external functional layer, a greater speed can be obtained. (For the SEM image of the smooth surface of the micromotor see Figure Figure 1 in the Supporting Information). Therefore, the movement speed of the micromotor Au/Ni/Ag is greater than the movement speed of the micromotor Cu/Ni/Ag. The catalytic performance of platinum is much better than that of silver.^[21] It can be seen from Figure 3 that the micromotor Au/Ni/Pt has the fastest speed among all types of micromotors. When the hydrogen peroxide concentration is 5%, it can reach $37.57 \mu\text{m/s}$.

Previous research by Wang showed that surfactants have an important influence on the size and separation of bubbles.^[12d] Next in this study, the concentration of H_2O_2 was fixed at 2% (Here, we take the lowest hydrogen peroxide concentration in the previous experiment as a fixed value) and the type of surfactant was changed. We choose Triton X-100, Tween 20 and Sodium dodecyl sulfate (SDS) as the comparison objects, and the concentrations are all set from 1% to 5%. The critical micelle concentrations (CMC) of these surfactants are 0.22 wt% (Triton X-100), 0.01 wt% (Tween 20), 0.24 wt% (SDS).^[22] The experimental results are shown in Figure 4. The movement speed of the microtubules is affected by the concentration of surfactant. When the concentration is less than 3%, the movement speed of the microtubules increases significantly. When the concentration exceeds 3%, the increasing trend of the movement speed begins to slow down. The three kinds of surfactants have slight differences in the promotion of microtubule movement speed, from the observation of experimental results, Triton X-100 has the best effect, followed by SDS, and then Tween 20, but they all show the same trend of change. Interfacial tension and fluid viscosity may be responsible for this phenomenon. Since the interfacial tension is already relatively constant at the CMC, an increase in the surfactant concentration does not have a significant effect on the interfacial tension.^[23] However, increasing surfactant concentration will inevitably increase the viscosity of the solution. According to the Stoke's equation, the velocity of microjets decreases with an increase in viscosity.^[12d] Therefore, after the concentration reaches 3%, the

further increase of surfactant concentration leads to the decrease of microjet velocity, which slows down the trend of increasing microtubule velocity. Therefore, blindly increasing the surfactant concentration is not a reliable method for increasing micromotors' speed.

In order to investigate the cargo transportation capacity of a three-layer tube motor, a single-layer tube made of inert Au was placed in aqueous H_2O_2 solution as the cargo needing to be transported (Gold does not react with hydrogen peroxide and can act as an immovable target in the solution, which is beneficial for the microtubes to contact the target under the guidance of an external magnetic field). Figure 5 demonstrates in detail the carrying process (the complete delivery process is recorded in Video S1 in the Supporting Information). When the motor was placed in the configured solution, it was guided by an external magnetic field to quickly make contact with the cargo. The micromotor during transportation shows a good propelling speed of approximately $6 \mu\text{m/s}$. The contact process is shown in Figure 5 a and b. After a period of transportation, the cargo was carried by the microtubes to the destination under magnetic guidance. The transportation process is shown in Figure 5 c and it is proved that the micromotors manufactured by the template electrodeposition method does have a good transport capacity.

The application of micromotors in environmental purification was also explored. Methylene blue (MB) is a cationic dye that is harmful to the environment, and H_2O_2 is a common oxidant that produces high levels of decomposition. Active hydroxyl radicals can be used for oxidative degradation of dyes.^[24] As previously reported, micromotors can catalyze the

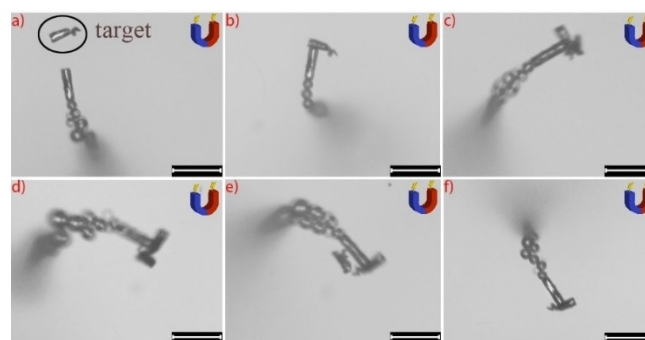


Figure 5. Track map of cargo transportation. (a) The microtubule approached to the target; (b) Contacted with the target (c–e) in transit; (f) Arrived at the destination (Scale bar: $20 \mu\text{m}$).

decomposition of H_2O_2 and produce a large number of active groups, such as HO_2^\bullet , $^\bullet\text{OH}$.^[25] These active groups use Fenton-like reactions to degrade methylene blue, and make MB decompose into MB radical material $\text{MB}(\text{OOH}^\bullet)$ ^[26] (As shown in Figure 6A). Au and Ag can become active sites for electron accumulation on motor surfaces and can help to catalyze H_2O_2 to produce hydroxyl radicals.^[27] In addition, the surface adsorption of bubbles generated by the catalysis of the micromotor and the micromixing caused by the movement of the micromotor may help to remove the dye.^[28] In this study, MB was the purification target, and two types of motors (Cu/Ni/Ag and Au/Ni/Ag) were selected as tools to enhance the catalytic H_2O_2 decomposition process.

In order to facilitate the observation of the color change of the solution, we have configured 30 ml of the solution in the same proportion in the glass beaker, take photos at specific time intervals after degradation has started and the result is shown in Figure 6B. The solution mixed with micromotors had obvious fading, and the effect was better than that of the natural catalytic degradation of pure H_2O_2 . After 2 hours, the degradation was basically completed. Figure 6C(a–c) shows the transmission spectra of MB solution in the three groups at specific time intervals, characterized by the transmission peak around 665 nm. According to the degradation rate calculation formula, $C = (T - T_0)/T$ (where T = Transmittance after adding micromotor, and T_0 = Transmittance without adding micromotors), Table 1 shows the degradation rate of these three time periods. It can be seen that after 2 hours, the degradation rate of the micromotor solution added with Au/Ni/Ag reached 85.8%. the degradation rate of the micromotor solution added

with Au/Ni/Ag reached 84.4%. Previous studies have shown that the efficiency of degrading Rhodamine-B^[29] is 76.82%. Here, our degradation efficiency has been improved to a certain extent, and both types of micromotors effectively enhance the degradation of methylene blue solution.

3. Conclusions

This study proved that a variety of metal tubular micromotors can be manufactured through a bottom-up method and have good motion rates. It demonstrates the advantages of electrochemical template method, which is economical and convenient, and can compound a variety of materials on a micromotor. Experiments have found that smooth surfaces and good catalytic materials can bring faster movement speeds under high hydrogen peroxide concentrations. There is a cut-off point for the influence of surfactant concentration on the speed of the micromotor, and the increase in speed beyond this value will no longer be obvious. This study also proved that the tubular micromotor has good cargo transportation capabilities. By adding micromotors to the methylene blue solution, the degradation is also better enhanced. Compared with previous studies,^[29] the degradation rate has also been improved. These results will help solve the problems associated with environmental pollution in the future.

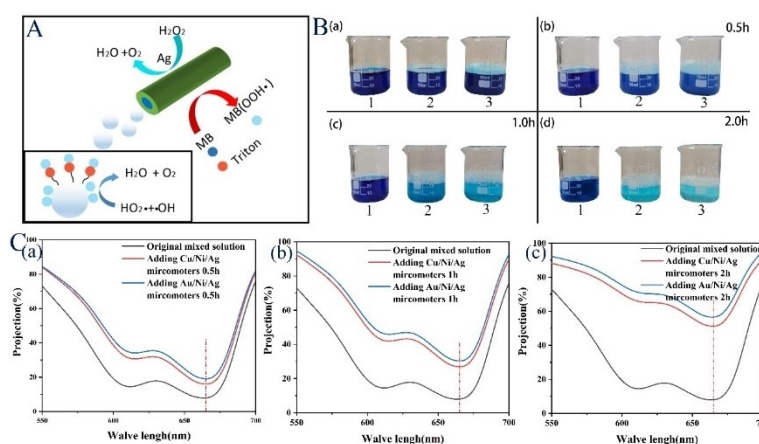


Figure 6. A. Schematic diagram of Fenton-like mechanism. B. Pictures of methylene blue degradation taken at a specific time. (a) Initiation stage of degradation (b) After half an hour of degradation (c) One hour after degradation (d) Two hours after degradation (The number 1 represents mixed solution of hydrogen peroxide and methylene blue, no microtubules in the solution. The number 2 represents the addition of Cu/Ni/Ag microtubules to the mixed solution. The number 3 represents the addition of Au/Ni/Ag microtubules to the mixed solution.) C. Transmissibility of three groups of experiments in different time periods. (a) After half an hour; (b) An hour later; (c) Two hours later; (The red dotted line represents the transmittance at 665 nm).

Table 1. Degradation rate in different time.

Time	0.5 h	1.0 h	2.0 h
Degradation rate of Au/Ni/Ag micromotors	58.1 %	73.7 %	85.8 %
Degradation rate of Cu/Ni/Ag micromotors	50.2 %	70.3 %	84.4 %
Degradation rate of Without micromotors		< 1 %	

Experimental Section

Materials

Non-ionic surfactants of Triton X-100 and Tween 20, and anionic surfactants of sodium dodecyl sulfate (SDS), $\text{H}_2\text{PtCl}_6 \cdot 6\text{H}_2\text{O}$, sulfuric acid (98% H_2SO_4), aniline, and sodium hydroxide (NaOH) were purchased from China Pharmaceutical Group Chemical Reagents Co., Ltd. Deionized water ($18.25 \text{ M}\Omega \times \text{cm}$) was obtained from a Millipore Milli-Q purification system. The Cyclopore polycarbonate membranes (Catalog no. 7060-2513), with an average pore diameter of $5 \mu\text{m}$, were purchased from Whatman Inc., NY, USA. All of the chemicals were of reagent grade and used without further treatment.

Characterization

Scanning electron microscopy (SEM) and energy-dispersive X-ray analysis were obtained by using a Hitachi S-4800 field-emission scanning electron microscope.

Preparation of Microtubes

The microtubes were prepared using a common template-directed electrodeposition protocol. The Cyclopore polycarbonate membranes were utilized as the templates. A 75 nm Au film was first sputtered on one side of the porous membrane to serve as working electrode using the DZ300 high vacuum single chamber thermal evaporation system. The evaporation was performed at room temperature under vacuum of 1×10^{-4} Torr. The membrane was then assembled in a plating cell with aluminum foil serving as a contact. Electrochemical deposition was carried out using a CHI 660E electrochemical workstation (CH Instruments Inc., Shanghai, China). A Pt wire was used as a counter electrode, and an Ag/AgCl with 3 M KCl was used as a reference electrode. PANI microtubes were electropolymerized at $+0.806 \text{ V}$ for 1 C from a plating solution that contained 0.1 M H_2SO_4 , 0.5 M Na_2SO_4 , and 0.1 M aniline; an intermediate Ni layer (essential for magnetic guidance) was deposited potentiostatically at -1.2 V for 3.8 C from the Ni plating mixture (a nickel solution that contained a mixture of 20 g/L $\text{NiCl}_2 \times 6\text{H}_2\text{O}$, 515 g/L $(\text{H}_2\text{NSO}_3)_2 \times 4\text{H}_2\text{O}$, and 20 g/L H_3BO_3).^[30] Subsequently, the inner Pt tube was deposited galvanostatically at -2 mA for 600 sec from a plating solution made of 0.01 M $\text{H}_2\text{PtCl}_6 \times 6\text{H}_2\text{O}$, 0.5 M H_2SO_4 . This resulted in a PANI/Pt micromotor with a Ni metal layer in the middle. Utilizing the same method, from a plating solution that contained 0.01 M $\text{HAuCl}_4 \times 4\text{H}_2\text{O}$ and 0.01 M H_3BO_3 , the Au layer was obtained by depositing at -2 mA for 300 sec under constant current. From a plating solution made of 0.02 M AgNO_3 and 0.02 M H_3BO_3 , the Ag layer was obtained by depositing at -2 mA for 600 sec under constant current. From a plating solution that contained 160 g/L $\text{CuSO}_4 \times 5\text{H}_2\text{O}$ and 20 g/L H_3BO_3 , while pH value was controlled at 2.5 , the Cu layer was obtained by depositing at -2 mA for 600 sec under constant current. The membrane was then stored for 24 h . The Au layer was completely removed by hand polishing with $5 \mu\text{m}$ alumina particles. The membrane was then dissolved in methylene chloride to release the micromotors. The micromotors were collected by centrifugation at 6000 rpm for 3 min while they were repeatedly washed with dichloromethane, ethanol, and ultrapure water three times each. All the micromotors were stored in ultrapure water at room temperature for further use.

Motion Investigations

An H_2O_2 droplet with different concentrations containing 1% Triton X-100 was placed on a glass slide. The height of the solution was approximately 3 mm . A vertical metallographic microscope (DYJ-980BD) was used to observe the spontaneous movement of micromotors in the solution. Images were then recorded with a CCD camera (DYS-500, DIANCAM). Video tracker software was used to analyze the motion trajectory of micromotor.

Degradation of MB

In order to evaluate whether the motor can promote the decomposition of H_2O_2 and achieve the purpose of rapid degradation of MB (MB, $\text{C}_{16}\text{H}_{18}\text{ClN}_3\text{S} \times 3\text{H}_2\text{O}$), two different types of micromotors (Cu/Ni/Ag and Au/Ni/Ag) were used. Measurements of the solution without micromotors, and the transmittance of the solution with micromotors, was measured by UV-VIS-NIR spectrophotometer (SHIMADZU, Japan). For the catalytic degradation experiments of MB (30 mg/L), one batch of micromotors ($\approx 2 \mu\text{L}$), $250 \mu\text{L}$ H_2O_2 solution (30%), and $250 \mu\text{L}$ Triton-X100 solution (1%) were configured into a 1 mL mixture. During the degradation, the reaction mixture was analyzed at specific time intervals after quick centrifugation to isolate the micromotors. The remaining concentration of MB in solution was calculated by measuring the transmittance at $\approx 664 \text{ nm}$.

Acknowledgements

This work was supported by the National Natural Science Foundation of China (Nos. 51502168; 11504227), Science and Technology Commission of Shanghai Municipality (19DZ2271100).

Conflict of Interest

The authors declare no conflict of interest.

Keywords: cargo transportation · catalytic materials · degradation · micromotors · template electrodeposition

- [1] a) Y. Mei, A. A. Solovev, S. Sanchez, O. G. Schmidt, *Chem. Soc. Rev.* **2011**, *40*, 2109–2119; b) A. Zenerino, C. Peyratout, A. Aimable, *J. Colloid Interface Sci.* **2015**, *450*, 174–181; c) H. Wang, M. Pumera, *Chem. Rev.* **2015**, *115*, 8704–8735; d) Y. Yu, L. Shang, W. Gao, Z. Zhao, H. Wang, Y. Zhao, *Angew. Chem. Int. Ed. Engl.* **2017**, *56*, 12127–12131.
- [2] J. G. S. Moo, C. C. Mayorga-Martinez, H. Wang, B. Khezri, W. Z. Teo, M. Pumera, *Adv. Funct. Mater.* **2017**, *27*, 1604759.
- [3] W. F. Paxton, K. C. Kistler, C. C. Olmeda, A. Sen, S. K. St. Angelo, Y. Cao, T. E. Mallouk, P. E. Lammert, V. H. Crespi, *J. Am. Chem. Soc.* **2004**, *126*, 13424–13431.
- [4] a) F. Ma, B. Xu, S. Wu, L. Wang, B. Zhang, G. Huang, A. Du, B. Zhou, Y. Mei, *Nanotechnology* **2019**, *30*, 354001; b) T. Komatsu, *Chem. Lett.* **2020**, *49*, 1245–1255.
- [5] W. G. A. J. Wang, *ACS Nano* **2014**, *8*, 3170–3180.
- [6] Y. Xia, P. Yang, Y. Sun, Y. Wu, B. Mayers, B. Gates, Y. Yin, F. Kim, H. Yan, *Adv. Mater.* **2003**, *15*, 353–389.
- [7] a) B. Zhang, G. Huang, L. Wang, T. Wang, L. Liu, Z. Di, X. Liu, Y. Mei, *Chem. Asian J.* **2019**, *14*, 2479–2484; b) M. Pacheco, M. Á. López, B. Jurado-Sánchez, A. Escarpa, *Anal. Bioanal. Chem.* **2019**, *411*, 6561–6573.
- [8] a) L. Ren, D. Zhou, Z. Mao, P. Xu, T. J. Huang, T. E. Mallouk, *ACS Nano* **2017**, *11*, 10591–10598; b) W. Wang, W. Duan, S. Ahmed, T. E. Mallouk, A. Sen, *Nano Today* **2013**, *8*, 531–554.

- [9] E. Harlev, T. Gulakhmedova, I. Rubinovich, G. Aizenshtein, *Adv. Mater.* **1996**, *8*, 994–997.
- [10] F. Novotný, J. Plutnar, M. Pumera, *Adv. Funct. Mater.* **2019**, *29*, 1903041.
- [11] a) Y. Mei, G. Huang, A. A. Solovev, E. B. Ureña, I. Mönch, F. Ding, T. Reindl, R. K. Y. Fu, P. K. Chu, O. G. Schmidt, *Adv. Mater.* **2008**, *20*, 4085–4090; b) D. Vilela, J. Parmar, Y. Zeng, Y. Zhao, S. Sanchez, *Nano Lett.* **2016**, *16*, 2860–2866; c) Z. Wu, X. Lin, Y. Wu, T. Si, J. Sun, Q. He, *ACS Nano* **2014**, *8*, 6097–6105; d) Y. Wu, Z. Wu, X. Lin, Q. He, J. Li, *ACS Nano* **2012**, *6*, 10910–10916.
- [12] a) G. Zhao, S. Sanchez, O. G. Schmidt, M. Pumera, *Nanoscale* **2013**, *5*, 2909–2914; b) L. Soler, V. Magdanz, V. M. Fomin, S. Sanchez, O. G. Schmidt, *ACS Nano* **2013**, *7*, 9611–9620; c) L. Soler, C. Martínez-Cisneros, A. Swiersy, S. Sanchez, O. G. Schmidt, *Lab Chip* **2013**, *13*, 4299–4303; d) H. Wang, G. J. Zhao, M. Pumera, *J. Phys. Chem. C* **2014**, *118*, 5268–5274; e) R. Mestre, N. Cadefau, A. C. Hortelao, J. Grzelak, M. Gich, A. Roig, S. Sanchez, *ChemNanoMat* **2021**, *7*, 134–140.
- [13] a) W. Wang, Z. Wu, X. Lin, T. Si, Q. He, *J. Am. Chem. Soc.* **2019**, *141*, 6601–6608; b) M. Safdar, J. Simmchen, J. Jänis, *Environ. Sci.-Nano* **2017**, *4*, 1602–1616; c) J. Katuri, X. Ma, M. M. Stanton, S. Sánchez, *Acc. Chem. Res.* **2017**, *50*, 2–11; d) Y. Wang, Z. Li, A. A. Solovev, G. Huang, Y. Mei, *RSC Adv.* **2019**, *9*, 29433–29439; e) L. J. Cai, H. Wang, Y. R. Yu, F. K. Bian, Y. Wang, K. Q. Shi, F. F. Ye, Y. J. Zhao, *Natl. Sci. Rev.* **2020**, *7*, 644–651.
- [14] Z. Li, Z. Li, Z. Xie, Y. Mei, Y. Wang, G. Huang, Y. Liu, *SN Applied Sciences* **2020**, *2*, 746–749.
- [15] A. Martín, B. Jurado-Sánchez, A. Escarpa, J. Wang, *Small* **2015**, *11*, 3568–3574.
- [16] F. Zha, T. Wang, M. Luo, J. Guan, *Micromachines* **2018**, *9*, 78.
- [17] L. Liu, T. Bai, Q. Chi, Z. Wang, S. Xu, Q. Liu, Q. Wang, *Micromachines* **2017**, *8*, 267–273.
- [18] S. E. Ilse, C. Holm, J. de Graaf, *J. Chem. Phys.* **2016**, *145*, 323.
- [19] N. F. Atta, A. Galal, F. M. Abdel-Gawad, E. F. Mohamed, *Electroanalysis* **2014**, *27*, 415–428.
- [20] M. O. Finot, G. D. Braybrook, M. T. McDermott, *J. Electroanal. Chem.* **1999**, *466*, 234–241.
- [21] a) J. Li, W. Liu, X. Wu, X. Gao, *Biomaterials* **2015**, *48*, 37–44; b) T. H. Oh, B. Jang, S. Kwon, *Int. J. Hydrogen Energy* **2014**, *39*, 6977–6986.
- [22] C. Kim, Y.-L. Hsieh, *Colloids Surf. A* **2001**, *187*, 385–397.
- [23] J. Simmchen, V. Magdanz, S. Sanchez, S. Chokmaviroj, D. Ruiz-Molina, A. Baeza, O. G. Schmidt, *RSC Adv.* **2014**, *4*, 20334–20340.
- [24] F. Gulshan, S. Yanagida, Y. Kameshima, T. Isobe, A. Nakajima, K. Okada, *Water Res.* **2010**, *44*, 2876–2884.
- [25] L. J. Liu, J. C. Yan, C. Zheng, R. Xiao, P. Q. Dai, Q. T. Wang, W. Li, W. Z. Chen, *NANO* **2020**, *15*, 12–17.
- [26] V. M. Lluís Soler, Vladimir M. Fomin, S. Sanchez, Oliver G. Schmidt, *ACS Nano* **2013**, *7*, 9611–9620.
- [27] a) K.-L. Zhang, X.-P. Lin, F.-Q. Huang, W.-D. Wang, *J. Mol. Catal. A* **2006**, *258*, 185–190; b) T. T. Y. Tan, C. K. Yip, D. Beydoun, R. Amal, *Chem. Eng. J.* **2003**, *95*, 179–186.
- [28] O. M. Wani, M. Safdar, N. Kinnunen, J. Janis, *Chem. Eur. J.* **2016**, *22*, 1244–1247.
- [29] F. Yu, Q. Hu, L. Dong, X. Cui, T. Chen, H. Xin, M. Liu, C. Xue, X. Song, F. Ai, T. Li, X. Wang, *Sci. Rep.* **2017**, *7*, 41169.
- [30] W. Gao, S. Sattayasamitsathit, A. Uygun, A. Pei, A. Ponedal, J. Wang, *Nanoscale* **2012**, *4*, 2447–2453.

Manuscript received: March 12, 2021

Revised manuscript received: June 7, 2021